

---

# Sharp Calibrated Gaussian Processes

---

Alexandre Capone<sup>1</sup> Geoff Pleiss<sup>2</sup> Sandra Hirche<sup>1</sup>

## Abstract

While Gaussian processes are a mainstay for various engineering and scientific applications, the uncertainty estimates don't satisfy frequentist guarantees, and can be miscalibrated in practice. State-of-the-art approaches for designing calibrated models rely on inflating the Gaussian process posterior variance, which yields confidence intervals that are potentially too coarse. To remedy this, we present a calibration approach that generates predictive quantiles using a computation inspired by the vanilla Gaussian process posterior variance, but using a different set of hyperparameters, chosen to satisfy an empirical calibration constraint. This results in a calibration approach that is considerably more flexible than existing approaches. Our approach is shown to yield a calibrated model under reasonable assumptions. Furthermore, it outperforms existing approaches not only when employed for calibrated regression, but also to inform the design of Bayesian optimization algorithms.

## 1. Introduction

Gaussian process regression offers an ambitious proposition: by conditioning a model on measurement data, we are provided with a Gaussian probability distribution for the unseen data. Assuming that the posterior probability distribution holds, we can then directly calibrate our model using the inverse error function. Though the distribution of unseen data seldom follows the Gaussian prior distribution, and the Gaussian process generally does not adapt adequately to the observed distributions after being conditioned on the data, Gaussian processes have become one of the most powerful and established regression techniques. Besides having found widespread use in machine learning (Deisenroth et al., 2015; Srinivas et al., 2012), their good

generalization properties have motivated applications in the fields of control (Capone & Hirche, 2019), astrophysics (Roberts et al., 2013) and chemistry (Deringer et al., 2021), to name a few. Furthermore, the Bayesian paradigm offers a powerful tool to analyze the theoretical properties of different regression techniques (Srinivas et al., 2012; Capone et al., 2022).

In this paper, we present a novel approach to obtaining calibrated Gaussian processes. Instead of computing confidence intervals by inflating the GP posterior variance, our approach discards it and computes a new quantity inspired by the computation of the posterior variance, where all hyperparameters are chosen in a way that results in both accurate and sharp calibration.

normally obtained with obtaining an alternative variance estimate using new hyperparameters. In other words, we train two separate Gaussian processes: one for the posterior mean and one for obtaining confidence intervals, posterior variance, which is exclusively used for calibration purposes. By doing so, we reach considerably more flexibility than existing calibration approaches, which enables us to additionally optimize the sharpness of the calibration. Our approach is shown to outperform vanilla Gaussian processes, fully Bayesian Gaussian processes, as well as a state-of-the-art calibration approach, both in terms of calibration and sharpness.

**Notation.** We use  $\mathbb{R}_+$  to denote the non-negative real numbers. Boldface lowercase/uppercase characters denote vectors/matrices. For two vectors  $\mathbf{a}$  and  $\mathbf{a}'$  in  $\mathbb{R}^d$ , we employ the notation  $\mathbf{a} \leq \mathbf{a}'$  to denote componentwise inequality, i.e.,  $a_i \leq a'_i, i = 1, \dots, d$ . For a square matrix  $\mathbf{K}$ , we use  $|\mathbf{K}|$  to denote its determinant, and  $[\mathbf{K}]_{ij}$  to denote the entry corresponding to the  $i$ -th row and  $j$ -th column.

## 2. Related Work

**Calibration of Classification Models.** There has been extensive work on obtaining calibrated models in the domain of classification. While there are many methods that do not employ post-processing, we only focus here on methods that employ some form of post-processing. Most forms post-processing-based calibration for classification fall into the category of conformal methods (Vovk et al.), which,

---

<sup>1</sup>School of Computation, Information and Technology, Technical University of Munich, Munich, Germany <sup>2</sup>Department of Statistics and Zuckerman Institute, Columbia University, New York, USA. Correspondence to: Alexandre Capone <alexandre.capone@tum.de>.

given an input, aim to produce sets of labels that contain the true label with a pre-specified probability. Arguably the two most common forms of calibration are isotonic regression (Niculescu-Mizil & Caruana, 2005) and Platt scaling (Platt et al., 1999). In Niculescu-Mizil & Caruana (2005), Platt scaling and isotonic regression are analyzed extensively for different types of predictive models. In Guo et al. (2017), a modified form of Platt scaling for modern classification neural networks is proposed.

**Calibration of Regression Models.** Though initially developed for classification, conformal calibration has been extended to regression settings. In Lakshminarayanan et al. (2017), a calibration approach was proposed for deep ensembles. Gal et al. (2017) propose a dropout-based technique for calibrating deep neural networks. However, these approaches require changing the regressor, potentially deteriorating its predictive performance. It should be noted that Bayesian neural networks (MacKay, 1995), while being able to provide credible sets for the output, they fully trust the posterior, resulting in a naively calibrated model that seldom reflects the data’s distribution. As a remedy for this, Kuleshov et al. (2018) present a recalibration approach that scales a model’s predictive quantiles to satisfy the observed data’s distribution. In Vovk et al. (2020), a similar approach is presented, where interpolation between scaling factors is randomized. An extension of both Kuleshov et al. (2018) and Vovk et al. (2020) and other recalibration is proposed in Marx et al. (2022). While these methods have been shown to yield well-calibrated models, the resulting predictive quantiles are potentially much too crude, resulting in predictions that perform poorly in terms of sharpness, i.e., the corresponding confidence intervals will overestimate the model error by a very large margin.

### 3. Problem Statement

Consider a compact input space  $\mathcal{X} \subset \mathbb{R}^d$  and output space  $\mathcal{Y} \subset \mathbb{R}$ , and an unknown data distribution  $\Pi$  on  $\mathcal{X} \times \mathcal{Y}$ . Given training data  $\mathcal{D} \sim \Pi$ , consider a model that, for every  $\mathbf{x} \in \mathcal{X}$  and confidence level  $\delta \in [0, 1]$ , returns a predictive mean  $\mu_{\mathcal{D}}(\delta, \mathbf{x})$ , posterior standard deviation  $\sigma_{\mathcal{D}}(\delta, \mathbf{x})$ , and scaling factor  $\beta_{\delta}$ . The model is then said to be calibrated if

$$\mathbb{P}_{\mathbf{x}, y \sim \Pi} \left( y - \mu_{\mathcal{D}}(\delta, \mathbf{x}) \leq \beta_{\delta} \sigma_{\mathcal{D}}(\delta, \mathbf{x}) \right) = \delta \quad (1)$$

holds for every  $\delta \in [0, 1]$ . Furthermore, the calibrated model is also said to be sharp if the average length of the predicted quantiles

$$\mathbb{E}_{\mathbf{x}, y \sim \Pi} (|\beta_{\delta} \sigma_{\mathcal{D}}(\delta, \mathbf{x})|)$$

is small for every  $\delta$  (Kuleshov et al., 2018). Our goal is to find a sharply calibrated model based on Gaussian process regression.

## 4. Gaussian Process Regression

In this section, we briefly review GP regression, with particular focus on the choice and influence of hyperparameters.

A GP is formally defined as a collection of random variables, any subset of which is jointly Gaussian (Rasmussen & Williams, 2006). It is fully specified by a prior mean function, which we set to zero without loss of generality, and a hyperparameter-dependent covariance function, called kernel  $k : \Theta \times \mathcal{X} \times \mathcal{X} \rightarrow \mathbb{R}$ , where  $\Theta$  denotes the hyperparameter space. The core concept behind GP regression lies in assuming that any finite number of measurements of an unknown function  $f : \mathcal{X} \rightarrow \mathbb{R}$  at arbitrary inputs  $\mathbf{x}_1, \dots, \mathbf{x}_N \in \mathcal{X}$  is drawn from a GP, i.e., they are jointly Gaussian with mean zero and covariance  $\mathbf{K}(\boldsymbol{\vartheta})$ , where

$$[\mathbf{K}(\boldsymbol{\vartheta})]_{ij} = k(\boldsymbol{\vartheta}, \mathbf{x}_i, \mathbf{x}_j)$$

consists of kernel evaluations at the test inputs.

Given a set of noisy observations  $\mathcal{D} = \{\mathbf{x}_i, y_i\}_{i=1}^N$ , where  $y_i := f(\mathbf{x}_i) + \varepsilon_i$  and  $\varepsilon_i \sim \mathcal{N}(0, \sigma_0^2)$  is iid Gaussian measurement noise, we can condition the GP on them to obtain the posterior mean and covariance

$$\mu_{\mathcal{D}}(\boldsymbol{\vartheta}, \mathbf{x}^*) = \mathbf{k}(\boldsymbol{\vartheta}) (\mathbf{K}(\boldsymbol{\vartheta}) + \sigma_0^2 \mathbf{I})^{-1} \mathbf{y}, \quad (2a)$$

$$\sigma_{\mathcal{D}}^2(\boldsymbol{\vartheta}, \mathbf{x}^*) = k(\boldsymbol{\vartheta}, \mathbf{x}^*, \mathbf{x}^*) - \mathbf{k}(\boldsymbol{\vartheta}) (\mathbf{K}(\boldsymbol{\vartheta}) + \sigma_0^2 \mathbf{I})^{-1} \mathbf{k}(\boldsymbol{\vartheta}), \quad (2b)$$

with  $\mathbf{k}(\boldsymbol{\vartheta}) := (k(\boldsymbol{\vartheta}, \mathbf{x}^*, \mathbf{x}_1), \dots, k(\boldsymbol{\vartheta}, \mathbf{x}^*, \mathbf{x}_N))$ ,  $\mathbf{y} = (y_1, \dots, y_N)$ , and  $\mathbf{I}$  denoting the identity matrix. In this paper, we restrict ourselves to kernels  $k(\cdot, \cdot, \cdot)$  that yield a posterior variance that is monotonically increasing with respect to the hyperparameters  $\boldsymbol{\vartheta}$ , as specified in the following assumption.

**Assumption 4.1.** The posterior variance  $\sigma^2(\boldsymbol{\vartheta}, \mathbf{x}^*)$  is a continuous function of  $\boldsymbol{\vartheta}$ . Furthermore, for all hyperparameters  $\boldsymbol{\vartheta}, \boldsymbol{\vartheta}' \in \Theta$  with  $\boldsymbol{\vartheta} \leq \boldsymbol{\vartheta}'$ , it holds that  $\sigma^2(\boldsymbol{\vartheta}, \mathbf{x}^*) \leq \sigma^2(\boldsymbol{\vartheta}', \mathbf{x}^*)$ .

Assumption 4.1 is not very restrictive, as it holds for many commonly used kernels, e.g., linear or isotropic kernels (Capone et al., 2022). Furthermore, it can also be enforced via a reparametrization of the kernel, e.g., if  $\boldsymbol{\vartheta}$  corresponds to the inverse of the lengthscales. Assumption 4.1 will be leveraged to define a cumulative density function by also changing the parameters of the posterior covariance, as opposed to simply scaling it.

Arguably one of the most challenging aspects of GP regression lies in the choice of hyperparameters  $\boldsymbol{\vartheta}$ , as they ultimately determine various characteristics of the posterior, e.g., smoothness and amplitude. In practice, the most common way of choosing  $\boldsymbol{\vartheta}$  is by minimizing the log marginal

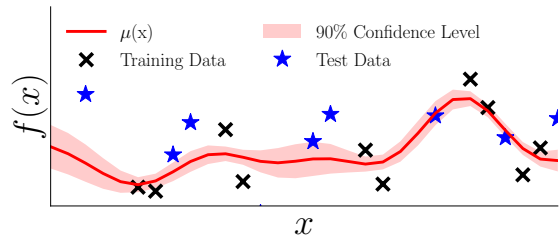


Figure 1. Confidence interval of 90% obtained with purely Bayesian approach, where the inverse error function is employed to compute  $\beta_\delta$ . The confidence region does not capture the training nor the test data with 90% accuracy, indicating that it is exceedingly confident.

likelihood

$$\begin{aligned} \log p(\mathbf{y}|\mathbf{X}, \boldsymbol{\vartheta}) &= -\frac{1}{2} \log |\mathbf{K}(\boldsymbol{\vartheta}) + \sigma_0^2 \mathbf{I}| \\ &\quad - \frac{N}{2} \log(2\pi) - \frac{1}{2} \mathbf{y}^\top (\mathbf{K}(\boldsymbol{\vartheta}) + \sigma_0^2 \mathbf{I})^{-1} \mathbf{y}. \end{aligned} \quad (3)$$

In terms of *posterior mean* quality, i.e., predictive performance of  $\mu(\boldsymbol{\vartheta}, \mathbf{x}^*)$ , choosing the hyperparameters in this manner is often the most promising option, since it seeks a trade-off between model complexity and data fit, and has repeatedly been shown to yield a satisfactory mean square error when applied to test data (Rasmussen & Williams, 2006). However, the same generally cannot be said of the posterior variance  $\sigma^2(\boldsymbol{\vartheta}, \mathbf{x}^*)$ , particularly whenever it is employed to estimate the model error, as it has been shown to be overly confident in practice (Capone et al., 2022; Fong & Holmes, 2020). This excess in confidence stems directly from the minimization of the log marginal likelihood (3), which measures the GP’s ability to explain the existing data, but not its ability to make predictions on unseen data (Lotfi et al., 2022). This is because, on the one hand, the log marginal likelihood (3) does not account for calibration, i.e., how well the posterior variance explains the model error. On the other hand, in practice the Gaussian prior for the data often deviates much too strongly from its true distribution, and the posterior, being also Gaussian, typically also presents a poor fit. This discrepancy between the posterior and the unseen data has serious implications for whenever we aim to obtain a calibrated model, i.e., a model that provides accurate confidence intervals for the unseen data. This is particularly true of the Bayesian approach to confidence intervals, where we obtain confidence intervals by simply multiplying the posterior standard deviation with expected the z-score, see Figure 1 for an illustration.

## 5. Proposed Approach

In this section, we present our approach to obtaining calibrated GPs by discarding the posterior variance and obtaining an alternative variance estimate using new hyperparameters. As we will demonstrate, our approach has numerous advantages. First, by modifying the posterior mean hyperparameters, the resulting variance and confidence intervals can be sharper than what could be obtained simply by rescaling the posterior variance. Secondly, by exploiting the monotonicity of hyperparameters, our approach can be used to obtain intervals for multiple confidence levels  $\delta$  in a very efficient manner. Finally, our method is backed by tight theoretical guarantees, obtained by exploiting its connection to conformal prediction.

### 5.1. Calibrated GP for Single Confidence Level $\delta$

In the following, we describe how to obtain a sharply calibrated GP for a fixed desired calibration level  $\delta$ . In this paper, we quantify sharpness using the measure suggested by Kuleshov et al. (2018), whereby a model is said to be sharp if the average posterior variance of the calibrated model is low. Instead of scaling the GP posterior variance to meet the desired calibration level  $\delta$ , we propose retraining the full posterior variance. In other words, we discard the posterior variance of the first GP and replace it by the posterior variance of a second GP, which we train separately. This way, we allow for more degrees of freedom during calibration, which enables for a more sharply calibrated model.

We assume to have a GP posterior mean  $\mu_{\mathcal{D}}(\boldsymbol{\vartheta}^R, \cdot)$ , where the regressor hyperparameters  $\boldsymbol{\vartheta}^R$  were obtained, e.g., via log-likelihood maximization. Choosing the hyperparameters for the posterior via log-likelihood maximization is typically promising due to the trade-off between data fit and model complexity discussed in Section 4. However, any other way of choosing  $\boldsymbol{\vartheta}^R$  is permitted, e.g., expert knowledge or by minimizing metrics that take generalization into account (Lotfi et al., 2022).

Given  $\boldsymbol{\vartheta}^R$ , we then aim to obtain, for an arbitrary  $0 \leq \delta \leq 1$ , a vector of hyperparameters  $\boldsymbol{\vartheta}_\delta$ , such that the corresponding posterior standard deviation  $\sigma_{\mathcal{D}}(\boldsymbol{\vartheta}_\delta, \cdot)$  contains  $\delta$  times the total amount of data points. For this reason, we henceforth refer to  $\boldsymbol{\vartheta}_\delta$  and  $\sigma_{\mathcal{D}_\text{tr}}^2(\boldsymbol{\vartheta}_\delta, \cdot)$  as *calibration hyperparameters* and *calibration variance*, respectively.

A naive way of choosing  $\beta_\delta$  and  $\boldsymbol{\vartheta}_\delta$  would be by guaranteeing that  $\beta_\delta \sigma_{\mathcal{D}_\text{tr}}(\boldsymbol{\vartheta}_\delta, \cdot)$  contains exactly  $\delta$  times the desired number of data from  $\mathcal{D}$ . While a similar approach might be reasonable, e.g., for Bayesian or ensemble neural networks, it should be avoided in the case of GPs. This is because  $\sigma_{\mathcal{D}_\text{tr}}(\boldsymbol{\vartheta}_\delta, \cdot)$  is approximately proportional to the measurement noise at  $\mathcal{D}$ , whereas it behaves considerably differently for test points that are not close to the data  $\mathcal{D}$ . Since we wish

to obtain a model that is calibrated within the whole input space  $\mathcal{X}$ , we have to take this into account during training. To this end, we randomly split the total available data  $\mathcal{D}$  into posterior variance training data  $\mathcal{D}_{\text{tr}}$  and calibration data  $\mathcal{D}_{\text{cal}}$ , with  $\mathcal{D} = \mathcal{D}_{\text{tr}} \cup \mathcal{D}_{\text{cal}}$ . The posterior mean  $\mu_{\mathcal{D}_{\text{tr}}}(\boldsymbol{\vartheta}^R, \cdot)$  and the calibration variance  $\sigma_{\mathcal{D}_{\text{tr}}}(\boldsymbol{\vartheta}_\delta, \cdot)$  are then conditioned uniquely on  $\mathcal{D}_{\text{tr}}$ , and  $\mathcal{D}_{\text{cal}}$  is employed to choose sharp calibration hyperparameters  $\boldsymbol{\vartheta}_\delta$ . To achieve this, we aim to solve the equation

$$\begin{aligned} \min_{\substack{\beta_\delta \in \mathbb{R} \\ \boldsymbol{\vartheta} \in \Theta}} & \sum_i^{N_{\text{cal}}} \beta_\delta^2 \sigma_{\mathcal{D}_{\text{tr}}}^2(\boldsymbol{\vartheta}_\delta, \mathbf{x}_{\text{cal}}^i) \\ \text{s.t.} & \sum_i^{N_{\text{cal}}} \frac{\mathbb{I}_{\geq 0}(\Delta y_{\text{cal}}^i - \beta_\delta \sigma_{\mathcal{D}_{\text{tr}}}(\boldsymbol{\vartheta}_\delta, \mathbf{x}_{\text{cal}}^i))}{N_{\text{cal}} + 1} = \delta \end{aligned} \quad (4)$$

for  $\boldsymbol{\vartheta}_\delta$ , where  $\{\mathbf{x}_{\text{cal}}^i, y_{\text{cal}}^i\} \in \mathcal{D}_{\text{cal}}$  are samples from the calibration data set,  $\Delta y_{\text{cal}}^i := y_{\text{cal}}^i - \mu_{\mathcal{D}_{\text{tr}}}(\boldsymbol{\vartheta}^R, \mathbf{x}_{\text{cal}}^i)$  corresponds to the difference between predicted and measured output,  $N_{\text{cal}} = |\mathcal{D}_{\text{cal}}|$  corresponds to the number of data points used for calibration.

*Remark 5.1.* Note that we employ  $N_{\text{cal}} + 1$  in the denominator in (4) instead of  $N_{\text{cal}}$ . Though this choice makes little difference in practice, we require it for theoretical guarantees.

The equality constraint in (4) is generally infeasible, e.g., if  $N_{\text{cal}} = 2$  and  $\delta = 0.5$ , and is discontinuous, making it hard to solve. As it turns out, this can be easily remedied, and the problem can be rendered considerably easier to solve, by substituting the equality constraint in (4) with the equality

$$\beta_\delta = q_{\text{lin}}(\delta, \boldsymbol{\Sigma}_{\mathcal{D}_{\text{tr}}}^{-1} \boldsymbol{\Delta} \mathbf{y}_{\text{cal}}), \quad (5)$$

where  $q_{\text{lin}}(\delta, \boldsymbol{\Sigma}_{\mathcal{D}_{\text{tr}}}^{-1} \boldsymbol{\Delta} \mathbf{y}_{\text{cal}})$  is a monotonically increasing piecewise linear function<sup>1</sup> that maps  $\delta = j/(N_{\text{cal}} + 1)$  to the  $j$ -th smallest entry of  $\boldsymbol{\Sigma}_{\mathcal{D}_{\text{tr}}}^{-1} \boldsymbol{\Delta} \mathbf{y}_{\text{cal}}$ , and the entries of the vector

$$\boldsymbol{\Sigma}_{\mathcal{D}_{\text{tr}}}^{-1} \boldsymbol{\Delta} \mathbf{y}_{\text{cal}} = \left( \frac{\Delta y_{\text{cal}}^1}{\sigma_{\mathcal{D}_{\text{tr}}}(\boldsymbol{\vartheta}_\delta, \mathbf{x}_{\text{cal}}^1)}, \dots, \frac{\Delta y_{\text{cal}}^{N_{\text{cal}}}}{\sigma_{\mathcal{D}_{\text{tr}}}(\boldsymbol{\vartheta}_\delta, \mathbf{x}_{\text{cal}}^{N_{\text{cal}}})} \right)^\top$$

correspond to the z-scores of the data under the calibration standard deviation  $\sigma_{\mathcal{D}_{\text{tr}}}(\boldsymbol{\vartheta}_\delta, \cdot)$ . The original problem (4) then becomes

$$\min_{\boldsymbol{\vartheta} \in \Theta} \sum_i^{N_{\text{cal}}} [q_{\text{lin}}(\delta, \boldsymbol{\Sigma}_{\mathcal{D}_{\text{tr}}}^{-1} \boldsymbol{\Delta} \mathbf{y}_{\text{cal}}) \sigma_{\mathcal{D}_{\text{tr}}}(\boldsymbol{\vartheta}_\delta, \mathbf{x}_{\text{cal}}^i)]^2, \quad (6)$$

<sup>1</sup>For  $\mathbf{a} \in \mathbb{R}^{N_{\text{cal}}}$ , a permutation  $i_1, \dots, i_{N_{\text{cal}}} \in [1, \dots, N_{\text{cal}}]$  where  $a_{i_j} \leq a_{i_{j+1}}$  for all  $j$ , and  $\delta \in [l/(N_{\text{cal}} + 1), (l + 1)/(N_{\text{cal}} + 1)]$ ,

$$q_{\text{lin}}(\delta, \mathbf{a}) = a_{i_l} + (\delta(N + 1) - l)(a_{i_{l+1}} - a_{i_l}).$$

---

### Algorithm 1 Training Calibration Hyperparameters for Arbitrary Confidence Level

---

**Input:** kernel  $k(\cdot, \cdot, \cdot)$ , predictor  $\mu(\boldsymbol{\vartheta}^R, \cdot)$ , calibration data  $\mathcal{D}_{\text{cal}}$ , confidence levels  $\delta_1, \dots, \delta_N$

**for**  $i = 1$  **to**  $M$  **do**

Compute  $\boldsymbol{\vartheta}_{\delta_i}$  and  $\beta_{\delta_i}$  by solving (6) subject to  $\boldsymbol{\vartheta}_{\delta_{i-1}} \leq \boldsymbol{\vartheta}_{\delta_i}$  if  $\beta_{\delta_i} > 0$  and  $\boldsymbol{\vartheta}_{\delta_{i-1}} \geq \boldsymbol{\vartheta}_{\delta_i}$  if  $\beta_{\delta_i} < 0$

**end for**

Fit a continuous, monotonically increasing interpolation model  $\hat{\beta}(\delta)$  and a continuous model  $\hat{\boldsymbol{\vartheta}}(\delta)$  using the training data  $\{\delta_i, \beta_{\delta_i}, \boldsymbol{\vartheta}_{\delta_i}\}_{i=1, \dots, N}$

**Output:**  $\hat{\boldsymbol{\vartheta}}(\delta)$

---

which is considerably easier to solve due to the lack of constraints, and enables us to use gradient-based approaches, since  $q_{\text{lin}}(\delta, \boldsymbol{\Sigma}_{\mathcal{D}_{\text{tr}}}^{-1} \boldsymbol{\Delta} \mathbf{y}_{\text{cal}})$  is differentiable with respect to  $\sigma_{\mathcal{D}_{\text{tr}}}(\boldsymbol{\vartheta}_\delta, \mathbf{x}_{\text{cal}}^i)$ .

## 5.2. Calibrated GP for Arbitrary Confidence Level $\delta$

While (6) is useful for obtaining a sharply calibrated model for a single confidence level  $\delta$ , solving (6) multiple times whenever we want to obtain sharply calibrated models for different confidence levels  $\delta$  can be time-consuming. Furthermore, interpolating between any two arbitrary solutions of (6) won't necessarily yield a result close to the desired calibration. Fortunately, we can leverage Assumption 4.1 to show that interpolating between two solutions of (6) will yield a result close to the desired calibration, provided that we interpolate between two strictly increasing or decreasing sets of hyperparameters. Formally, this is achieved by solving (6)  $N + 1$  times to obtain  $\beta_0, \beta_{\delta_1}, \dots, \beta_{\delta_N} \in \mathbb{R}$  and  $\boldsymbol{\vartheta}_0, \boldsymbol{\vartheta}_{\delta_1}, \dots, \boldsymbol{\vartheta}_{\delta_N} \in \mathbb{R}$ , subject to two additional constraints. Firstly, the calibration scaling parameters  $\beta_\delta$  must be monotonically increasing with  $\delta$ , i.e.,

$$\beta_{\delta_i} \leq \beta_{\delta_j} \quad \text{if } \delta_i < \delta_j,$$

and the calibration hyperparameters  $\boldsymbol{\vartheta}_\delta$  must be decreasing with  $\delta$  if  $\beta_\delta$  is negative, and increasing if  $\beta_\delta$  is positive, i.e.,

$$\boldsymbol{\vartheta}_{\delta_i} \leq \boldsymbol{\vartheta}_{\delta_j}, \quad \text{if } \delta_i < \delta_j \text{ and } \beta_i \geq 0,$$

$$\boldsymbol{\vartheta}_{\delta_i} \geq \boldsymbol{\vartheta}_{\delta_j}, \quad \text{if } \delta_i < \delta_j \text{ and } \beta_j \leq 0.$$

In other words, the entries of  $\boldsymbol{\vartheta}_\delta$  are strictly decreasing with  $\beta_\delta$  up until the sign of  $\beta_\delta$  switches, after which they are increasing. The reason why we impose these restrictions is that we can then confidently interpolate between any values of  $\beta_\delta$  and  $\boldsymbol{\vartheta}_\delta$ , since Assumption 4.1 implies that the quantile stipulated by  $\beta_\delta \sigma(\boldsymbol{\vartheta}, \cdot)$  is monotonically increasing with  $\delta$ . We then train simple linear interpolation models  $\hat{\beta} : [0, 1] \rightarrow \mathbb{R}$  and  $\hat{\boldsymbol{\vartheta}} : [0, 1] \rightarrow \Theta$ , such that  $\hat{\beta}(\delta_i) = \beta_{\delta_i}$  and  $\hat{\boldsymbol{\vartheta}}(\delta_i) = \boldsymbol{\vartheta}_{\delta_i}$ , with the additional constraint that  $\hat{\boldsymbol{\vartheta}}(\delta)$

reaches a minimum whenever  $\hat{\beta}(\delta) = 0$ , which can be potentially achieved by adding an artificial vector of training hyperparameters  $\vartheta_\delta$  for computing  $\hat{\vartheta}(\delta)$ . Note, however, that any other form of interpolation is also acceptable for obtaining  $\hat{\beta}(\delta)$  and  $\hat{\vartheta}(\delta)$ .

*Remark 5.2.* While lengthscale constraints of the form  $\vartheta_{\delta_j} \leq \vartheta_{\delta_{j+1}}$  can be easily enforced when solving (6) by substituting  $\vartheta$  with  $\vartheta_{\delta_j} + \Delta\vartheta$  and minimizing over the logarithm of  $\Delta\vartheta$ , the constraint  $\beta_{\delta_j} \leq \beta_{\delta_{j+1}}$  is not enforced in (6). However, in practice we were often able to find local minima of (6) that satisfy this requirement.

We can then easily show that our approach achieves an arbitrary calibration level as the amount of data grows provided that we choose the confidence levels  $\delta$  accordingly.

**Theorem 5.3.** *Let  $y$  be absolutely continuous conditioned on  $\mathbf{x}$ , let  $\mu_{\mathcal{D}_r}(\vartheta^R, \cdot)$  be a posterior GP mean, and let  $\sigma_{\mathcal{D}_r}(\cdot, \cdot)$  be a GP posterior variance conditioned on  $\mathcal{D}_r$ . Then, for any calibration data set  $\mathcal{D}_{cal} = \{\mathbf{x}_{cal}^i, y_{cal}^i\}$ , choose*

$$\delta_1 = \frac{1}{N_{cal} + 1}, \delta_2 = \frac{2}{N_{cal} + 1}, \dots, \delta_{N_{cal}} = \frac{N_{cal}}{N_{cal} + 1}$$

*$\beta_{\delta_1}, \dots, \beta_{\delta_{N_{cal}}} \in \mathbb{R}$  be  $N_{cal}$  scalars and  $\vartheta_{\delta_1}, \dots, \vartheta_{\delta_{N_{cal}}} \in \Theta$  be  $N_{cal}$  vectors of calibration hyperparameters, such that  $\beta_{\delta_1} \leq \dots \leq \beta_{\delta_{N_{cal}}}$  and*

$$\begin{aligned} \vartheta_{\delta_{i-1}} &\geq \vartheta_{\delta_i} && \text{if } \beta_{\delta_i} \leq 0 \\ \vartheta_{\delta_i} &\leq \vartheta_{\delta_{i+1}} && \text{if } \beta_{\delta_i} \geq 0. \end{aligned}$$

Then

$$\begin{aligned} &\mathbb{P}_{\mathbf{x}, y \sim \Pi} \left( y - \mu_{\mathcal{D}_r}(\hat{\vartheta}(\delta), \mathbf{x}) \leq \hat{\beta}(\delta) \sigma_{\mathcal{D}_r}(\hat{\vartheta}(\delta), \mathbf{x}) \right) \\ &\in \left[ \delta - \frac{1}{N_{cal} + 1}, \delta + \frac{1}{N_{cal} + 1} \right]. \end{aligned}$$

*Proof.* The proof can be found in Appendix A.  $\square$

Note that Theorem 5.3 also implies that a single set of calibration parameters  $\beta_\delta$  and  $\vartheta_\delta$  obtained by solving (6), since we can substitute  $\hat{\beta}(\delta) = \beta_\delta$  and  $\hat{\vartheta}(\delta) = \vartheta_\delta$  into (7).

## 6. Discussion

**Computational Complexity.** There are many ways to alleviate the computational cost of our approach. Much like hyperparameter optimization for standard GPs (Rasmussen & Williams, 2006), we can employ only a subset of the data  $\mathcal{D}$  to choose the calibration variances, and afterwards the full data set for predictions. This reduces the cost of inverting the covariance matrix significantly, as the cost of inversion scales cubically. Note that our technique is also readily applicable to sparse GPs. Moreover, in many settings

a specific level of calibration is often required, as opposed to several different ones, e.g., in stochastic model predictive control, where chance constraints corresponding to a fixed risk have to be satisfied (Mesbah, 2016). In such settings, we potentially only have to train a single vector of calibration hyperparameters  $\vartheta_\delta$ , which reduces computational cost.

**Initialization and Solution.** Much like in standard GP hyperparameter training, the choice of initial hyperparameters can affect the optimization results considerably, and choosing a good hyperparameter initialization can be challenging. While this can be partially addressed by employing random restarts, we can also reuse trained models for similar calibration levels, since it is reasonable to expect that only small changes to the hyperparameters are required to achieve a slight increase or decrease in confidence level. Furthermore, we can also simplify the problem by considering only a scaled version of the regression hyperparameters  $\vartheta^R$  to compute  $\vartheta_\delta$ , which would reduce the optimization problem to a line search.

## 7. Experiments

In this section, we apply and analyze our approach in regression and Bayesian optimization settings.

### 7.1. Calibrated Regression

We begin with numerical regression experiments, where the goal is to obtain a calibrated regression model. We test our approach on various data sets and compare it to the state-of-the-art recalibration approaches by Kuleshov et al. (2018) and Vovk et al. (2020), the variance-free approach proposed by Marx et al. (2022), as well as the naive Bayesian approach for the vanilla and fully Bayesian GPs. The technique proposed by Kuleshov et al. (2018) essentially scales the posterior standard deviation such that the confidence level observed on the training data matches that of the desired confidence level. Vovk et al. (2020) employ a similar approach, except that random interpolation is employed to compute new scaling values, while the variance-free approach proposed in Marx et al. (2022) simply computes a constant and uses it to bound the model error everywhere. In the two Bayesian approaches, the credible sets are assumed to correspond exactly to confidence intervals. In all approaches, we employ a squared-exponential kernel and a prior mean of zero, except for datasets with more than 1000 training data points, where we employ sparse GPs (Titsias, 2009) with 300 inducing points.

#### 7.1.1. TOY DATA SET

The first regression data set corresponds to a one-dimensional version of the Ackley function, where the results can be easily displayed visually. The main purpose of

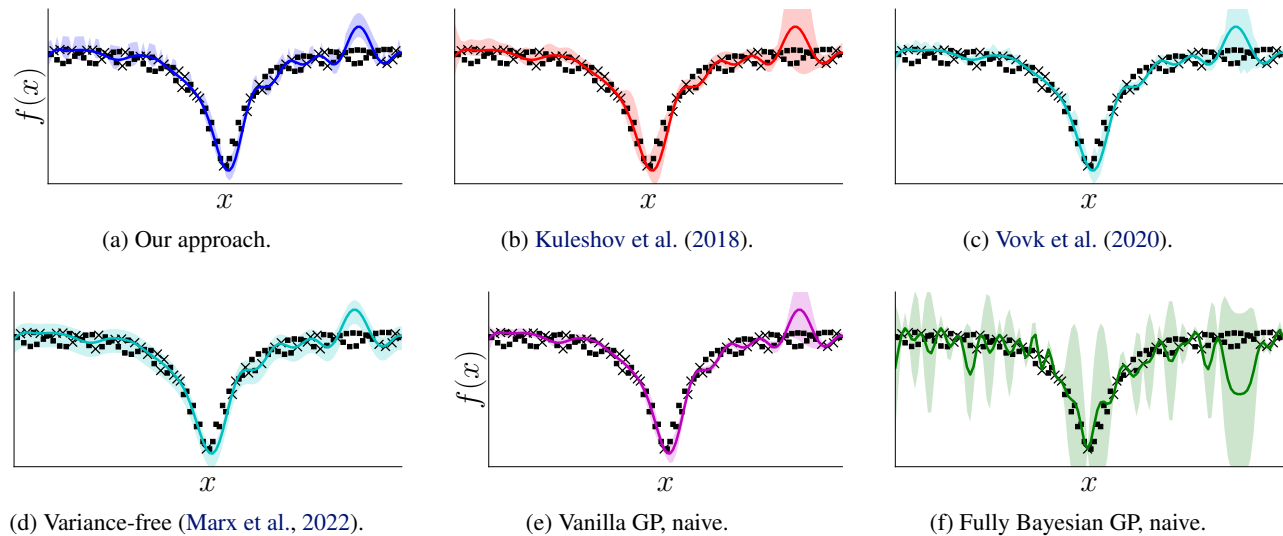


Figure 2. Calibrated regression models obtained with a desired calibration of  $\delta = 0.01f$  and our method (blue), a vanilla GP rescaled using the approach by Kuleshov et al. (2018), a naive vanilla GP (green), and a naive fully Bayesian GP (magenta). Compared to the other approaches, our approach yields a calibrated model that peaks more significantly far away from the data while staying tight when close to the data. This is because of the added flexibility that comes from being able to also change the lengthscale to design a calibrated model.

Table 1. Average expected calibration error (7), scaled with a factor of 100 for ease of exposition, for six different approaches: ours, vanillas GP recalibrated using the methods of Kuleshov et al. (2018) (V-RK), Vovk et al. (2020) (V-RV) and the variance-free approach proposed in Marx et al. (2022) (V-RM), and naive (not recalibrated) vanilla and fully Bayesian Gaussian processes. Lower is better.

	BOSTON	YACHT	AUTO	WINE	CEMENT	KIN8NM	FACEBOOK2
OURS	0.376± 0.52	0.91 ± 1.5	0.36 ± 0.41	<b>0.072 ± 0.082</b>	<b>0.19 ± 0.18</b>	0.015 ± 0.026	<b>0.037 ± 0.091</b>
V-RK	<b>0.35± 0.53</b>	<b>0.86± 1.5</b>	<b>0.35± 0.46</b>	0.076± 0.091	0.23± 0.2	<b>0.014± 0.023</b>	0.038± 0.091
V-RV	<b>0.35± 0.53</b>	<b>0.86± 1.5</b>	0.36± 0.47	0.074± 0.088	0.037± 0.091	0.23± 0.2	<b>0.037± 0.091</b>
V-RM	0.55± 0.87	0.033± 0.046	1.5± 1.6	0.28± 0.41	2.2± 1.9	0.016± 0.025	0.04± 0.09
V	7.1± 21	6.8± 22	5.1± 22	5.4± 22	6.1± 22	0.76± 0.67	3.7± 4
FULLB	-	6.9± 21	7.1± 22	-	-	-	-

this section is to give an intuition as to how our approach approaches the computation of confidence intervals compared to other approaches. We investigate the performance of our approach and compare it to that of other approaches when employed to compute centered 99% confidence intervals. We observe that the confidence intervals obtained with our approach peak more sharply far away from the data while being considerably tighter near the data compared to other approaches. This is because we allow the lengthscale to decrease in order to obtain a calibration model, whereas the other approaches simply scale the posterior variance without changing any hyperparameters. The results are depicted in Figure 2.

### 7.1.2. BENCHMARK DATA SETS

We now experiment with different regression data sets from the UCI repository. We assess performance by employing

the diagnostic tools for calibration and sharpness proposed by Kuleshov et al. (2018) and Marx et al. (2022). The score used to quantify the quality of a forecast calibration is the (normalized) calibration error

$$\text{cal}(\mu_{\mathcal{D}}(\boldsymbol{\vartheta}^R, \cdot), \beta, \sigma_{\mathcal{D}_w}(\cdot, \cdot)) = \sum_{j=1}^m (p_j - \hat{p}_j)^2, \quad (7)$$

where  $p_j$  corresponds to the  $j$ -th desired confidence level, chosen, e.g., uniformly distributed between 0 and 1, and  $\hat{p}_j$  is the observed confidence level, i.e.,

$$\hat{p}_j = \frac{|\{y_t^* \mid \Delta y_t^* \leq \beta_{p_j} \sigma_{\mathcal{D}_w}(\boldsymbol{\vartheta}_{p_j} \mathbf{x}_t^*), t = 1, \dots, T\}|}{T}. \quad (8)$$

Here the superscript  $*$  denotes test inputs and outputs,  $T$  denotes the total number of test points, and  $\Delta y_t^* := \mu_{\mathcal{D}_w}(\boldsymbol{\vartheta}^R, \mathbf{x}_t^*) - y_t^*$ . To measure sharpness, we employ three

Table 2. Average quantile length (7) obtained our approach, vanilla GP recalibrated using the methods of Kuleshov et al. (2018) (V-RK), Vovk et al. (2020) (V-RV). We do not report the sharpness obtained with all other approaches, as they do not achieve good calibration as per Table 1, which makes sharpness meaningless. We report the mean value of the metric shown in (9). Lower is better.

DATA SET	BOSTON	YACHT	AUTO	WINE	CEMENT	KIN8NM	FACEBOOK2
OURS	<b>0.14 ± 0.2</b>	<b>0.33 ± 0.55</b>	<b>0.17 ± 0.28</b>	<b>2.1 ± 3.5</b>	<b>0.59 ± 0.73</b>	<b>0.031 ± 0.065</b>	<b>34 ± 160</b>
V-RK	0.36 ± 1.2	0.46 ± 0.89	0.25 ± 0.53	9.6 ± 27	0.68 ± 1	0.047 ± 0.12	41 ± 200
V-RV	0.36 ± 1.2	0.46 ± 0.89	0.24 ± 0.53	9.6 ± 27	0.68 ± 1	0.047 ± 0.12	41 ± 200
V-RM	0.42 ± 1.2	0.87 ± 1.4	0.55 ± 0.64	2 ± 6.3	1.7 ± 1.5	0.034 ± 0.072	43 ± 200

Table 3. Average length of centered 95% confidence interval obtained with our approach and vanilla GPs recalibrated using the methods of Kuleshov et al. (2018) (V-RK), Vovk et al. (2020) (V-RV) and the variance-free approach proposed in Marx et al. (2022) (V-RM). We do not report results obtained with other methods, as they do not achieve good calibration as per Table 1. Lower is better.

DATA SET	BOSTON	YACHT	AUTO	WINE	CEMENT	KIN8NM	FACEBOOK2
OURS	<b>1.2 ± 0.14</b>	1.8 ± 0.26	1.4 ± 0.19	<b>4.7 ± 0.35</b>	2.5 ± 0.04	0.47 ± 0.025	1.7 ± 0.13
V-RK	1.9 ± 0.41	2.3 ± 0.33	1.8 ± 0.25	8.7 ± 1.9	2.9 ± 0.044	0.47 ± 0.014	1.8 ± 0.15
V-RV	1.4 ± 0.24	2.2 ± 0.42	1.7 ± 0.23	6.1 ± 0.66	2.5 ± 0.086	0.47 ± 0.014	1.8 ± 0.15
V-RM	2 ± 0.58	<b>1.2 ± 0.12</b>	<b>0.89 ± 0.11</b>	7.2 ± 1.2	<b>1.5 ± 0.2</b>	<b>0.091 ± 0.0032</b>	<b>0.9 ± 0.09</b>

different quantities, two of which were proposed by Marx et al. (2022). The first one is the average square length of the quantile, given by

$$\text{len}(\beta_{\cdot}, \sigma_{\mathcal{D}_t}(\cdot, \cdot)) = \sum_{j=1}^m \sum_{t=1}^T \beta_{p_j}^2 \sigma_{\mathcal{D}}^2(\vartheta_{p_j}, \mathbf{x}_j^*). \quad (9)$$

The two other metrics correspond to the average length of the 95% confidence interval and the average negative log likelihood of the predictions.

When applying the approach of Kuleshov et al. (2018), the vanilla and fully Bayesian GPs, the quantile  $\beta_{\delta} \sigma(\vartheta_{p_j}, \mathbf{x}_j^*)$  in (7) and (9) are substituted by the corresponding posterior standard deviation multiplied by the (recalibrated) z-score. Similarly, Vovk et al. (2020) recalibrates the z-score using random interpolation, whereas the variance-free approach proposed in Marx et al. (2022) replaces  $\beta_{\delta} \sigma(\vartheta_{p_j}, \mathbf{x}_j^*)$  with a constant for all  $\mathbf{x}_j^*$ .

In Table 1 and Table 4, we report the calibration and sharpness, as given by (7) and (9), respectively.

As can be seen, our approach performs either marginally worse and or better in terms of expected calibration error compared to other existing calibration approaches. However, it consistently performs considerably better than every other approach in terms sharpness, average length of 95% confidence intervals, and negative log likelihood.

A general conclusion that we may draw from the results is that, in most settings, increasing sharpness, as measured by (9), is detrimental for calibration and vice-versa. This makes sense, since in many settings the calibration variance must be high in order to capture correspondingly high errors.

## 7.2. Bayesian Optimization

We now investigate how the proposed calibration approach can be employed in a Bayesian optimization context using two commonly used benchmark functions, the Ackley and Rosenbrock functions.

In Bayesian optimization, the goal is to find a point in input space that maximizes an unknown function  $f(\cdot)$ . In particular, we investigate how our calibrated GP bound performs when it is used as an upper confidence bound (UCB) for a GP-UCB type acquisition function. Simply put, given a data set  $\mathcal{D}_t$  of size  $t$ , the GP-UCB algorithm chooses a query point by maximizing the acquisition function

$$\mathbf{x}_{t+1}^* = \arg \max_{\mathbf{x}} \mu_{\mathcal{D}_t}(\vartheta^R, \mathbf{x}) + \beta_{\mathcal{D}_t} \sigma_{\mathcal{D}_t}(\vartheta^R, \mathbf{x}), \quad (10)$$

where  $\beta_{\mathcal{D}_t}$  is a tuning parameter that stipulates the trade-off between exploration and exploitation, and may or may not depend on the data set  $\mathcal{D}_t$ . It has been shown that, if the unknown function  $f(\cdot)$  belongs to the RKHS associated with the kernel  $k(\vartheta^R, \cdot, \cdot)$ , and  $\beta_{\mathcal{D}_t}$  is chosen sufficiently large, then the GP-UCB achieves sublinear regret (Chowdhury & Gopalan, 2017). However, both assumptions typically cannot be verified in practice, and choosing both the kernel  $k(\vartheta^R, \cdot, \cdot)$  and the scaling factor  $\beta_{\mathcal{D}_t}$  in a principled manner remains an open problem. We propose employing the modified acquisition function

$$\mathbf{x}^* = \arg \max_{\mathbf{x}} \mu_{\mathcal{D}_t}(\vartheta^R, \mathbf{x}) + \beta_{\delta} \sigma_{\mathcal{D}_t}(\vartheta_{\delta}, \mathbf{x}), \quad (11)$$

where the hyperparameters  $\vartheta_{\delta}$  are obtained via a calibrated model and a suitable choice of confidence parameter  $\delta$ . In the experiments, we set  $\beta_{\mathcal{D}_t} = 1$  and compute the calibrated hyperparameters by setting  $\delta = 0.01$ , meaning that we set

Table 4. Average negative log likelihood obtained with our approaches and vanilla GPs recalibrated using the methods of Kuleshov et al. (2018) (V-RK), Vovk et al. (2020) (V-RV) and the variance-free approach proposed in Marx et al. (2022) (V-RM). We do not report results obtained with all other approaches, as they do not achieve good calibration as per Table 1, which makes NLL meaningless. Lower is better.

DATA SET	BOSTON	YACHT	AUTO	WINE	CEMENT	KIN8NM	FACEBOOK2
OURS	<b>0.14 ± 0.13</b>	<b>0.44 ± 0.25</b>	<b>0.46 ± 0.055</b>	<b>1.4 ± 0.073</b>	<b>0.91 ± 0.043</b>	<b>-0.66 ± 0.036</b>	<b>-1.2 ± 0.01</b>
V-RK	0.36 ± 0.11	0.74 ± 0.074	0.58 ± 0.095	1.5 ± 0.068	1 ± 0.046	-0.64 ± 0.049	<b>-1.2 ± 0.01</b>
V-RV	0.74 ± 0.14	1.4 ± 0.18	1 ± 0.16	1.7 ± 0.073	1 ± 0.032	-0.63 ± 0.049	<b>-1.2 ± 0.02</b>
V-RM	0.39 ± 0.086	1.5 ± 0.17	0.97 ± 0.071	1.5 ± 0.12	1.5 ± 0.012	-0.63 ± 0.038	-1.1 ± 0.02

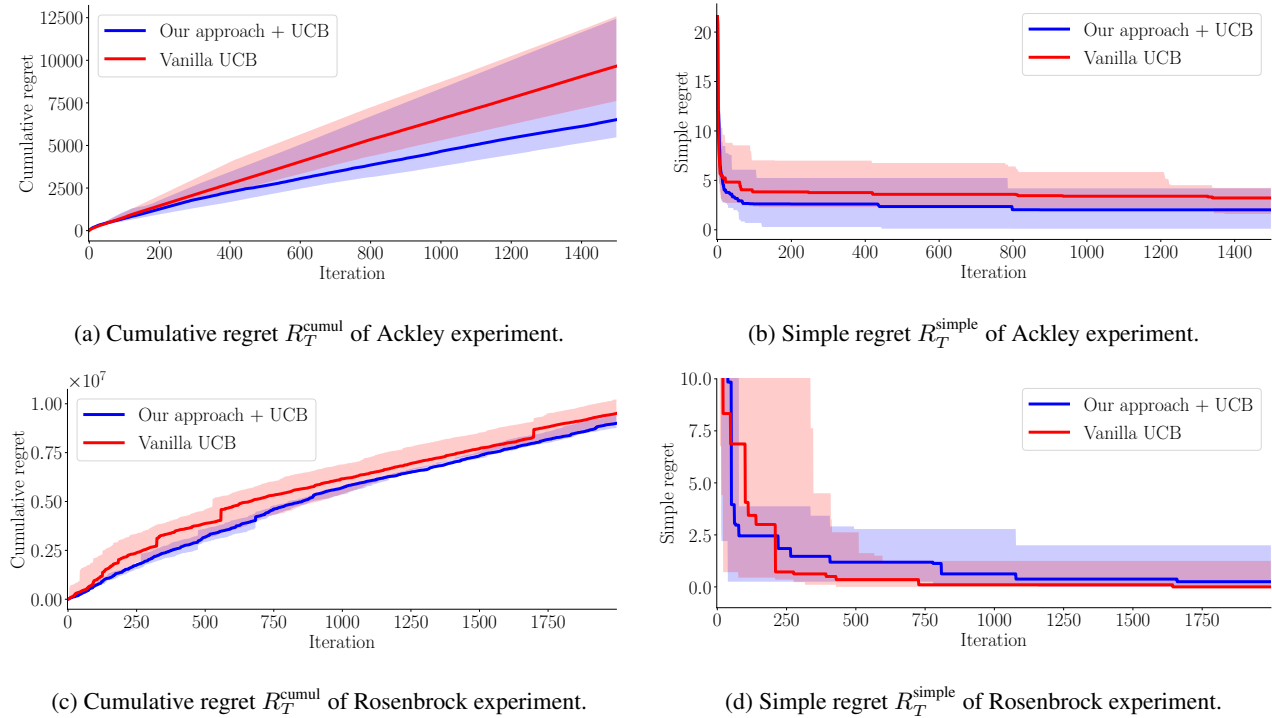


Figure 3. Regret of Ackley (top) and Rosenbrock (bottom) experiment over the number of Bayesian optimization iterations with UCB.

expect only one-percent of the evaluations to lie outside the confidence region. Note that, even though the underlying function is fixed, it is reasonable to expect that some of the data lies outside the confidence region due to noise, and we can only expect the data to lie fully within the confidence region in the noiseless case, which we do not consider in this paper. We additionally compare our results to the vanilla UCB algorithm, where the hyperparameters, chosen via log-likelihood maximization, are identical for both the posterior mean and variance, and we set  $\beta_{\mathcal{D}_t} = 2$ .

We evaluate the results both in terms of cumulative regret and simple regret. Cumulative regret after  $T$  steps corresponds to the metric

$$R_T^{\text{cumul}} = \sum_{t=1}^T \left( \max_{\mathbf{x} \in \mathcal{X}} f(\mathbf{x}) - f(\mathbf{x}_t) \right), \quad (12)$$

whereas simple regret is given by

$$R_T^{\text{simple}} = \max_{\mathbf{x} \in \mathcal{X}} f(\mathbf{x}) - \max_{t \leq T} f(\mathbf{x}_t). \quad (13)$$

Typically, a Bayesian optimization algorithm is deemed to be useful if cumulative regret exhibits sublinear growth, as this implies that the average regret goes to zero. Simple regret, by contrast, corresponds to the best query among all past queries.

In the case of the Ackley experiment, our approach typically chose lengthscales that were smaller than those computed via likelihood maximization. This results in more exhaustive exploration than vanilla UCB, which in turn means that local minima are explored more carefully before the focus of the optimization is shifted elsewhere. This results in performance, both in terms of cumulative and simple regret. The results correspond to the top two figures in Figure 3.



In contrast to the Ackley experiment, in the Rosenbrock experiment our approach selects lengthscales that are larger than those suggested by the likelihood maximum. Roughly speaking, this means that the confidence intervals produced by the likelihood maximum hyperparameters are too conservative, and our approach attempts to compensate this by indicating more confidence in the posterior mean obtained with the vanilla GP. This means that local minima are explored less meticulously than with the vanilla UCB algorithm. This choice is justified by the cumulative regret obtained with our approach, as it is slightly smaller than that obtained by the vanilla UCB algorithm. However, this also results in worse simple regret than the vanilla UCB algorithm, which is intuitive, as our approach opts to explore local minima less accurately than the vanilla UCB algorithm. We also note that both algorithms converge towards the same simple regret as the number of iterations increases.

## 8. Conclusion

We have presented a calibration method for Gaussian process regression that leverages monotonicity properties of the posterior lengthscale to obtain sharp calibrated models. We show that, under reasonable assumptions, our method yields an accurately calibrated model as the size of data used for calibration increases. When applied to different regression benchmark data sets, our approach always yielded more accurately calibrated models than other approaches, while being sharper than a state-of-the-art recalibration method. Furthermore, when employed to design an upper confidence bound Bayesian optimization algorithm, our approach resulted in better cumulative regret than the most commonly used approach.

## References

- Capone, A. and Hirche, S. Backstepping for partially unknown nonlinear systems using Gaussian processes. *IEEE Control Systems Letters*, 3:416–421, 2019.
- Capone, A., Lederer, A., and Hirche, S. Gaussian process uniform error bounds with unknown hyperparameters for safety-critical applications. In Chaudhuri, K., Jegelka, S., Song, L., Szepesvari, C., Niu, G., and Sabato, S. (eds.), *Proceedings of the 39th International Conference on Machine Learning*, volume 162 of *Proceedings of Machine Learning Research*, pp. 2609–2624. PMLR, 17–23 Jul 2022. URL <https://proceedings.mlr.press/v162/capone22a.html>.
- Chowdhury, S. R. and Gopalan, A. On kernelized multi-armed bandits. *arXiv preprint arXiv:1704.00445*, 2017.
- Deisenroth, M. P., Fox, D., and Rasmussen, C. E. Gaussian processes for data-efficient learning in robotics and control. *IEEE Transactions on Pattern Analysis and Machine Intelligence*, 37(2):408–423, 2015.
- Deringer, V. L., Bartók, A. P., Bernstein, N., Wilkins, D. M., Ceriotti, M., and Csányi, G. Gaussian process regression for materials and molecules. *Chemical Reviews*, 121(16):10073–10141, 2021. doi: 10.1021/acs.chemrev.1c00022. URL <https://doi.org/10.1021/acs.chemrev.1c00022>. PMID: 34398616.
- Fong, E. and Holmes, C. C. On the marginal likelihood and cross-validation. *Biometrika*, 107(2):489–496, 01 2020. ISSN 0006-3444. doi: 10.1093/biomet/asz077. URL <https://doi.org/10.1093/biomet/asz077>.
- Gal, Y., Hron, J., and Kendall, A. Concrete dropout. In Guyon, I., Luxburg, U. V., Bengio, S., Wallach, H., Fergus, R., Vishwanathan, S., and Garnett, R. (eds.), *Advances in Neural Information Processing Systems*, volume 30. Curran Associates, Inc., 2017. URL <https://proceedings.neurips.cc/paper/2017/file/84ddfb34126fc3a48ee38d7044e87276-Paper.pdf>.
- Guo, C., Pleiss, G., Sun, Y., and Weinberger, K. Q. On calibration of modern neural networks. In Precup, D. and Teh, Y. W. (eds.), *Proceedings of the 34th International Conference on Machine Learning*, volume 70 of *Proceedings of Machine Learning Research*, pp. 1321–1330. PMLR, 06–11 Aug 2017. URL <https://proceedings.mlr.press/v70/guo17a.html>.
- Kuleshov, V., Fenner, N., and Ermon, S. Accurate uncertainties for deep learning using calibrated regression. In *International Conference on Machine Learning*, pp. 2796–2804. PMLR, 2018.
- Lakshminarayanan, B., Pritzel, A., and Blundell, C. Simple and scalable predictive uncertainty estimation using deep ensembles. In Guyon, I., Luxburg, U. V., Bengio, S., Wallach, H., Fergus, R., Vishwanathan, S., and Garnett, R. (eds.), *Advances in Neural Information Processing Systems*, volume 30. Curran Associates, Inc., 2017. URL <https://proceedings.neurips.cc/paper/2017/file/9ef2ed4b7fd2c810847ffa5fa85bce38-Paper.pdf>.
- Lotfi, S., Izmailov, P., Benton, G., Goldblum, M., and Wilson, A. G. Bayesian model selection, the marginal likelihood, and generalization. In Chaudhuri, K., Jegelka, S., Song, L., Szepesvari, C., Niu, G., and Sabato, S. (eds.), *Proceedings of the 39th International Conference on Machine Learning*, volume 162 of *Proceedings of Machine Learning Research*, pp. 14223–14247. PMLR, 17–23 Jul

2022. URL <https://proceedings.mlr.press/v162/lotfi22a.html>.
- MacKay, D. J. Bayesian neural networks and density networks. *Nuclear Instruments and Methods in Physics Research Section A: Accelerators, Spectrometers, Detectors and Associated Equipment*, 354(1):73–80, 1995.
- Marx, C., Zhao, S., Neiswanger, W., and Ermon, S. Modular conformal calibration. In Chaudhuri, K., Jegelka, S., Song, L., Szepesvari, C., Niu, G., and Sabato, S. (eds.), *Proceedings of the 39th International Conference on Machine Learning*, volume 162 of *Proceedings of Machine Learning Research*, pp. 15180–15195. PMLR, 17–23 Jul 2022. URL <https://proceedings.mlr.press/v162/marx22a.html>.
- Mesbah, A. Stochastic model predictive control: An overview and perspectives for future research. *IEEE Control Systems Magazine*, 36(6):30–44, 2016.
- Niculescu-Mizil, A. and Caruana, R. Predicting good probabilities with supervised learning. New York, NY, USA, 2005. Association for Computing Machinery. ISBN 1595931805. URL <https://doi.org/10.1145/1102351.1102430>.
- Platt, J. et al. Probabilistic outputs for support vector machines and comparisons to regularized likelihood methods. *Advances in large margin classifiers*, 10(3):61–74, 1999.
- Rasmussen, C. E. and Williams, C. K. Gaussian processes for machine learning, 2006. *The MIT Press, Cambridge, MA, USA*, 2006.
- Roberts, S., Osborne, M., Ebden, M., Reece, S., Gibson, N., and Aigrain, S. Gaussian processes for time-series modelling. *Philosophical Transactions of the Royal Society A: Mathematical, Physical and Engineering Sciences*, 371(1984):20110550, 2013.
- Srinivas, N., Krause, A., Kakade, S. M., and Seeger, M. W. Information-theoretic regret bounds for Gaussian process optimization in the bandit setting. *IEEE Transactions on Information Theory*, 58(5):3250–3265, 2012.
- Titsias, M. Variational learning of inducing variables in sparse Gaussian processes. In *Artificial Intelligence and Statistics*, pp. 567–574, 2009.
- Vovk, V., Gammerman, A., and Shafer, G. *Algorithmic learning in a random world*, volume 29. Springer.
- Vovk, V., Petej, I., Toccaceli, P., Gammerman, A., Ahlberg, E., and Carlsson, L. Conformal calibrators. In Gammerman, A., Vovk, V., Luo, Z., Smirnov, E., and Cherubin, G. (eds.), *Proceedings of the Ninth Symposium on Conformal and Probabilistic Prediction and Applications*, volume 128 of *Proceedings of Machine Learning Research*, pp. 84–99. PMLR, 09–11 Sep 2020. URL <https://proceedings.mlr.press/v128/vovk20a.html>.

## A. Proof of Theorem 5.3

For the sake of completeness, we state Theorem 1 from Marx et al. (2022) here in adapted form, which we then use to prove Theorem 5.3.

**Lemma A.1** (Marx et al. (2022), Theorem 1). *Let  $\varphi : \mathcal{X} \times \mathbb{R} \rightarrow \mathbb{R}$  be a function such that  $\varphi(\mathbf{x}, y)$ ,  $\mathbf{x}, y \sim \Pi$  is an absolutely continuous random variable and, for any fixed  $\mathbf{x}^* \in \mathcal{X}$ ,  $\varphi(\mathbf{x}^*, \cdot)$  is strictly monotonically increasing. Furthermore, for a set of calibration data  $\mathcal{D}_{cal} = \{\mathbf{x}_{cal}^i, y_{cal}^i\}$  with  $N_{cal} = |\mathcal{D}_{cal}|$  and a permutation  $i_1, \dots, i_{N_{cal}} \in [1, 2, \dots, N_{cal}]$  such that*

$$\varphi(\mathbf{x}_{cal}^{i_j}, y_{cal}^{i_j}) < \varphi(\mathbf{x}_{cal}^{i_{j+1}}, y_{cal}^{i_{j+1}}),$$

let  $H : \mathbb{R} \rightarrow [0, 1]$  be a monotonically non-decreasing function, such that  $H(\varphi(\mathbf{x}_{cal}^{i_j}, y_{cal}^{i_j})) = \frac{j}{N_{cal}+1}$  holds for all  $j = 1, \dots, N_{cal}$ . Then

$$\mathbb{P}_{\mathbf{x}, y \sim \Pi} \left( H(\varphi(\mathbf{x}, y)) \leq \delta \right) \in \left[ \delta - \frac{1}{N_{cal}+1}, \delta + \frac{1}{N_{cal}+1} \right] \quad \forall \delta \in [0, 1].$$

The idea behind the proof of Theorem 5.3 is to show that the solution  $\varphi(\mathbf{x}, y)$  of the implicit equation

$$y - \mu(\boldsymbol{\vartheta}^R, \mathbf{x}) - \hat{\beta}(\varphi(\mathbf{x}, y))\sigma \left( \hat{\boldsymbol{\vartheta}}(\varphi(\mathbf{x}, y)), \mathbf{x} \right) = 0 \quad (14)$$

satisfies the requirements stipulated by Lemma A.1, where  $\tilde{\beta}(\delta)$  and  $\tilde{\boldsymbol{\vartheta}}(\delta)$  are arbitrary continuous functions such that

$$\begin{aligned} \lim_{\delta \rightarrow \infty} \tilde{\beta}(\delta) &= \infty, & \lim_{\delta \rightarrow -\infty} \tilde{\beta}(\delta) &= -\infty, \\ \lim_{\delta \rightarrow \infty} \tilde{\boldsymbol{\vartheta}}(\delta) &= \infty, & \lim_{\delta \rightarrow -\infty} \tilde{\boldsymbol{\vartheta}}(\delta) &= \infty, \end{aligned} \quad (15)$$

$$\begin{aligned} \tilde{\beta}(\delta) &\text{ is strictly monotonically increasing for all } \delta \in \mathbb{R} \\ \tilde{\boldsymbol{\vartheta}}(\delta) &\text{ is monotonically increasing for all } \delta \in \{\delta \in \mathbb{R} \mid \tilde{\beta}(\delta) > 0\} \\ \tilde{\boldsymbol{\vartheta}}(\delta) &\text{ is monotonically decreasing for all } \delta \in \{\delta \in \mathbb{R} \mid \tilde{\beta}(\delta) < 0\}. \end{aligned} \quad (16)$$

$\tilde{\boldsymbol{\vartheta}}(\delta)$  is monotonically increasing with respect to  $\delta$  for all  $\delta \in \{\delta \in \mathbb{R} \mid \tilde{\beta}(\delta) > 0\}$ , and monotonically decreasing with respect to  $\delta$  for all  $\delta \in \{\delta \in \mathbb{R} \mid \tilde{\beta}(\delta) < 0\}$ . Note that the functions  $\hat{\beta}(\delta)$  and  $\hat{\boldsymbol{\vartheta}}(\delta)$  can be easily extended within the real axis to satisfy the requirements mentioned above, which means that they are contained within the set from which  $\tilde{\beta}(\delta)$  and  $\tilde{\boldsymbol{\vartheta}}(\delta)$ . The reason why we choose arbitrary  $\tilde{\beta}(\delta)$  and  $\tilde{\boldsymbol{\vartheta}}(\delta)$ , as opposed to the functions  $\hat{\beta}(\delta)$  and  $\hat{\boldsymbol{\vartheta}}(\delta)$ , is because we need  $\varphi(\mathbf{x}, y)$  to be independent of the calibration data  $\mathcal{D}_{cal}$  in order to be able to employ Lemma A.1. Showing that  $\varphi(\mathbf{x}, y)$  satisfies the requirements of Lemma A.1 for any  $\tilde{\beta}(\delta)$  and  $\tilde{\boldsymbol{\vartheta}}(\delta)$  then implies that we can also choose any function within this class that minimizes sharpness, meaning that these properties also extend to  $\hat{\beta}(\delta)$  and  $\hat{\boldsymbol{\vartheta}}(\delta)$ .

To achieve prove Theorem 5.3, we will require the following result.

**Lemma A.2.** *Consider the regressor  $\mu(\boldsymbol{\vartheta}^R, \cdot)$ , and let  $\tilde{\beta}(\delta)$  and  $\tilde{\boldsymbol{\vartheta}}(\delta)$  be functions that satisfy (15) and (16). Then, for arbitrary fixed  $y$  and  $\mathbf{x}$ ,*

$$y - \mu(\boldsymbol{\vartheta}^R, \mathbf{x}) - \tilde{\beta}(\delta)\sigma \left( \tilde{\boldsymbol{\vartheta}}(\delta), \mathbf{x} \right) \quad (17)$$

is strictly monotonically decreasing with  $\delta$ .

*Proof.* The proof follows directly from Assumption 4.1 and the properties (15) and (16).  $\square$

*Proof of Theorem 5.3.* Let  $\tilde{\beta}(\delta)$  and  $\tilde{\boldsymbol{\vartheta}}(\delta)$  be functions that satisfy (15) and (16). Due to Lemma A.2, we can define the function  $\varphi : \mathcal{X} \times \mathbb{R} \rightarrow [0, 1]$  as the unique solution to the implicit equation

$$y - \mu(\boldsymbol{\vartheta}^R, \mathbf{x}) - \tilde{\beta}(\varphi(\mathbf{x}, y))\sigma \left( \tilde{\boldsymbol{\vartheta}}(\varphi(\mathbf{x}, y)), \mathbf{x} \right) = 0. \quad (18)$$

Note that, since  $y - \mu(\boldsymbol{\vartheta}^R, \mathbf{x})$  is strictly monotonically increasing with  $y$ ,  $\varphi(\mathbf{x}, y)$  is a strictly monotonically increasing function of  $y$  for any fixed  $\mathbf{x}$ . Furthermore, since  $y$  is absolutely continuous,

$$y_{\text{cal}}^i - \mu(\boldsymbol{\vartheta}^R, \mathbf{x}_{\text{cal}}^i) \neq y_{\text{cal}}^j - \mu(\boldsymbol{\vartheta}^R, \mathbf{x}_{\text{cal}}^j)$$

holds for all  $i \neq j$  almost surely, which implies  $\varphi(\mathbf{x}_{\text{cal}}^i, y_{\text{cal}}^i) \neq \varphi(\mathbf{x}_{\text{cal}}^j, y_{\text{cal}}^j)$  for all  $i \neq j$  almost surely. Hence,  $\varphi(\mathbf{x}, y)$ ,  $\mathbf{x}, y \sim \Pi$ , corresponds to an absolutely continuous random variable. Hence, given any monotonically non-decreasing function  $H(\cdot)$  that satisfies the requirement

$$H\left(\varphi(\mathbf{x}_{\text{cal}}^{i_j}, y_{\text{cal}}^{i_j})\right) = \frac{j}{N_{\text{cal}} + 1},$$

Lemma A.1 implies that

$$\mathbb{P}_{\mathbf{x}, y \sim \Pi} \left( H(\varphi(\mathbf{x}, y)) \leq \delta \right) \in \left[ \delta - \frac{1}{N_{\text{cal}} + 1}, \delta + \frac{1}{N_{\text{cal}} + 1} \right] \quad \forall \delta \in [0, 1]. \quad (19)$$

Since  $\tilde{\beta}(\delta)$  and  $\hat{\boldsymbol{\vartheta}}(\delta)$  are arbitrary, and  $\hat{\beta}(\delta)$  and  $\tilde{\boldsymbol{\vartheta}}(\delta)$  are continuous and also satisfy (15) and (16) within  $\delta \in [0, 1]$ , we can substitute  $\varphi(\cdot, \cdot)$  in (19) with  $\hat{\varphi}(\cdot, \cdot)$ , which is the unique solution of the implicit equation

$$y - \mu(\boldsymbol{\vartheta}^R, \mathbf{x}) - \hat{\beta}(\hat{\varphi}(\mathbf{x}, y))\sigma\left(\hat{\boldsymbol{\vartheta}}(\hat{\varphi}(\mathbf{x}, y)), \mathbf{x}\right) = 0. \quad (20)$$

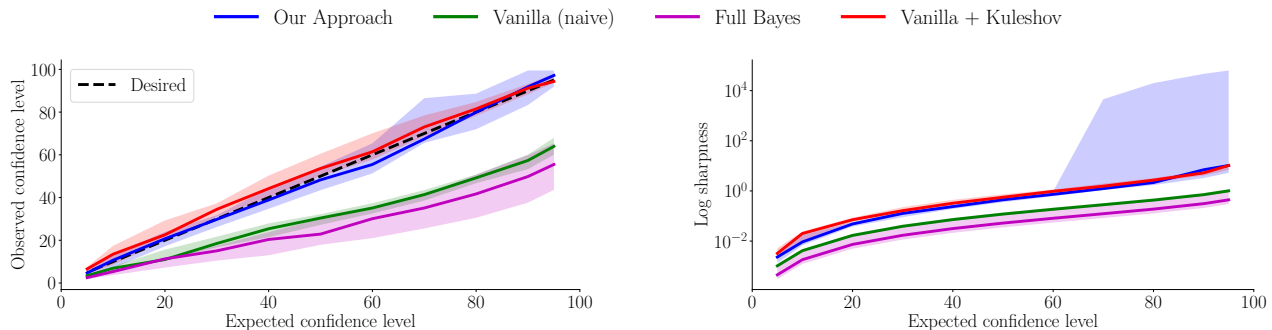
Now, in the particular case of  $\hat{\varphi}(\cdot, \cdot)$ , due to (6), we have that

$$\hat{\varphi}(\mathbf{x}_{\text{cal}}^{i_j}, y_{\text{cal}}^{i_j}) = \frac{j}{N_{\text{cal}} + 1},$$

meaning that  $H(\hat{\varphi}(\mathbf{x}_{\text{cal}}^{i_j}, y_{\text{cal}}^{i_j})) = \hat{\varphi}(\mathbf{x}_{\text{cal}}^{i_j}, y_{\text{cal}}^{i_j})$ , i.e., (19) holds for  $\varphi(\cdot, \cdot) = \hat{\varphi}(\cdot, \cdot)$  and the identity function  $H(\delta) = \delta$ . Furthermore, since  $\hat{\varphi}(\cdot, \cdot)$  is uniquely defined by the implicit equation (20) and  $\hat{\beta}(\delta)\sigma(\hat{\boldsymbol{\vartheta}}(\delta), \mathbf{x})$  is monotonically increasing with  $\delta$ , this in turn implies

$$\begin{aligned} \mathbb{P}_{\mathbf{x}, y \sim \Pi} \left( \hat{\varphi}(\mathbf{x}, y) \leq \delta \right) &= \mathbb{P}_{\mathbf{x}, y \sim \Pi} \left( \tilde{\beta}(\hat{\varphi}(\mathbf{x}, y))\sigma\left(\tilde{\boldsymbol{\vartheta}}(\hat{\varphi}(\mathbf{x}, y)), \mathbf{x}\right) \leq \tilde{\beta}(\delta)\sigma\left(\tilde{\boldsymbol{\vartheta}}(\delta), \mathbf{x}\right) \right) \\ &= \mathbb{P}_{\mathbf{x}, y \sim \Pi} \left( y - \mu(\boldsymbol{\vartheta}^R, \mathbf{x}) \leq \tilde{\beta}(\delta)\sigma\left(\tilde{\boldsymbol{\vartheta}}(\delta), \mathbf{x}\right) \right). \end{aligned}$$

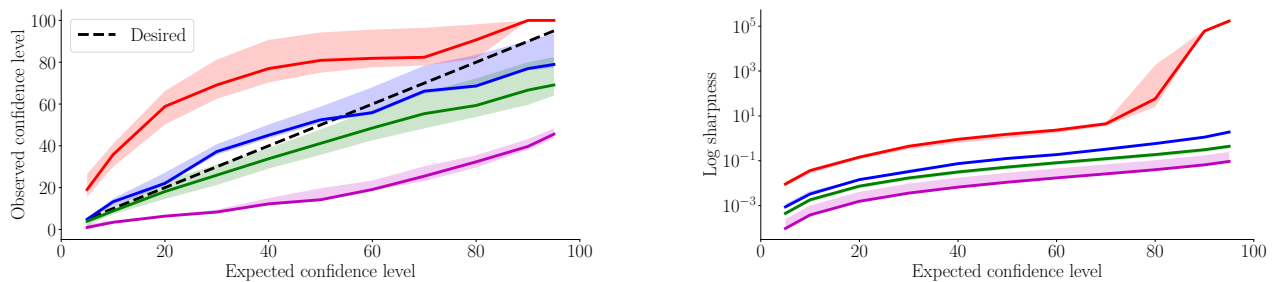
Since  $\tilde{\beta}(\delta)$  and  $\hat{\boldsymbol{\vartheta}}(\delta)$  are arbitrary, and  $\hat{\beta}(\delta)$  and  $\tilde{\boldsymbol{\vartheta}}(\delta)$  which, together with (19), implies the desired result. □



(a) Observed confidence level over expected rate of constraint satisfaction.

(b) Logarithm of sharpness over expected rate of constraint satisfaction.

Figure 4. Detailed results for wine data set.



(a) Observed confidence level over expected rate of constraint satisfaction.

(b) Logarithm of sharpness over expected rate of constraint satisfaction.

Figure 5. Detailed results for cement data set.

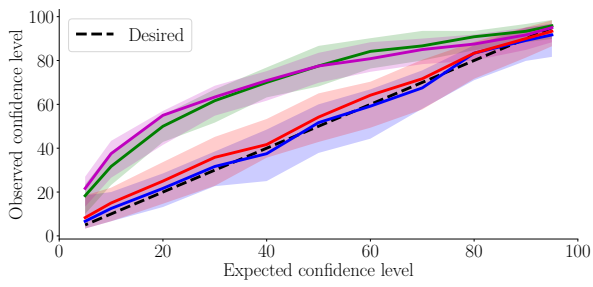
## B. Extended Experimental Section

In Figure 4, we plot results for the Boston house price data sets. More specifically, in Figure 4a, we plot the observed confidence level  $\hat{p}_j$ , as given by (8), over the desired confidence level  $p_j$ , and, in Figure 5b, the sharpness metric

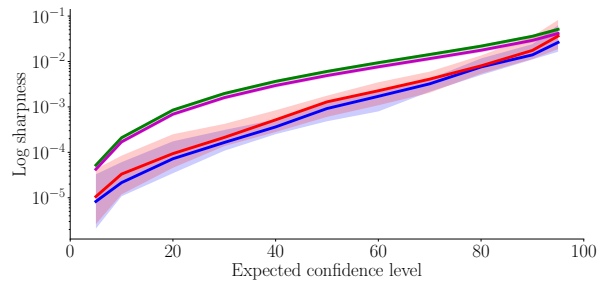
$$\sum_{t=1}^T \beta_{p_j}^2 \sigma_{\mathcal{D}_t}^2(\vartheta_{p_j}, \mathbf{x}_t^*),$$

over  $p_j$ .

Here we present graphs containing the detailed calibration and sharpness results for each experiment performed in Section 7.1.2.



(a) Observed confidence level over expected rate of constraint satisfaction.



(b) Logarithm of sharpness over expected rate of constraint satisfaction.

Figure 6. Detailed results for cement data set.